

FGF Binding and FGF Receptor Activation by Synthetic Heparan-Derived Di- and Trisaccharides

David M. Ornitz,* Andrew B. Herr, Marianne Nilsson, Jacob Westman, Carl-Magnus Svahn, Gabriel Waksman*

Fibroblast growth factors (FGFs) require a polysaccharide cofactor, heparin or heparan sulfate (HS), for receptor binding and activation. To probe the molecular mechanism by which heparin or HS (heparin/HS) activates FGF, small nonsulfated oligosaccharides found within heparin/HS were assayed for activity. These synthetic and isomerically pure compounds can activate the FGF signaling pathway. The crystal structures of complexes between FGF and these heparin/HS oligosaccharides reveal several binding sites on FGF and constrain possible mechanisms by which heparin/HS can activate the FGF receptor. These studies establish a framework for the molecular design of compounds capable of modulating FGF activity.

FGFs regulate a diverse range of physiologic processes such as cell growth and differentiation as well as pathologic processes involving angiogenesis, wound healing, and cancer (1). FGFs use a dual receptor system to activate signal transduction pathways (2–5). The primary component of this system is a family of signal-transducing FGF receptors (FGFRs) that contain an extracellular ligand-binding domain and an intracellular tyrosine kinase domain (1). The second component of this receptor system consists of HS proteoglycans or related heparin-like molecules that are required in order for FGF to bind to and activate the FGFR (3, 4). Although the mechanism by which heparin/HS activates FGF is unknown, heparin, FGF, and the FGFR can form a trimolecular complex (3). Heparin/HS may interact directly with the FGFR linking it to FGF (6). Furthermore, heparin/HS can facilitate the oligomerization of two or more FGF molecules, which may be important for receptor dimerization and activation (3). There are no pharmacologic agents that modulate the activity of FGFs.

Heparin and HS are heterogeneously sulfated glycosaminoglycans that consist of a repeating disaccharide unit of hexuronic acid and D-glucosamine. At a minimum, highly sulfated octa- (3) or decasaccharide (7) fragments derived from heparin are required for FGF to bind to the FGFR. However, preparation of these heparin fragments produces mixtures of isomers and chemically modifies the oligosaccharide ends (8). Furthermore, size-fractionated heparin may

contain individual molecules with distinct biological properties. To overcome these limitations and to address the question of whether nonsulfated oligosaccharide sequences, which are abundant in HS, are involved in FGFR activation, we have chemically synthesized and assayed the function of di-, tri-, and tetrasaccharides that correspond to structures found in heparin/HS (Table 1) (9). These heparin/HS analogs are isomerically pure and do not contain any modified sugar residues.

The F32 cell line, which expresses FGFR 1, requires heparin/HS and FGF for growth (3). This cell line was used to assay synthetic heparin/HS molecules as potential activators or inhibitors of heparin/HS-dependent mitogenesis (3). Two trisaccharides, Tri-1 and Tri-3, are active at concentrations comparable to that of heparin (Fig. 1 and Table 2). The third trisaccharide, Tri-2 (containing a glucosamine *N*-sulfate), and four disaccharides (Di-2, -3, -4, and -5) showed intermediate mitogenic activity with basic FGF (bFGF), whereas the disaccharide Di-1 and the three tetrasaccharides examined demonstrated no activity in this assay. Sucrose octasulfate (SOS), a highly

charged molecule thought to stabilize and activate bFGF (10), was also examined. Heparin, Tri-1, and Tri-3 were more than 1000 times more active than was SOS for F32 cell growth. Di-3 and -4 were 55 times more active in this assay.

Unlike previously examined fragments of heparin, several of these synthetic heparin/HS molecules are nonsulfated, yet they still have biological activity. Furthermore, they are considerably smaller than the smallest heparin oligosaccharide previously shown to activate FGF (3). Because several of these synthetic oligosaccharides are nonsulfated, interactions with the carbohydrate backbone of heparin/HS appear to be sufficient for biological activity. Furthermore, the large differences in activity observed between closely related oligosaccharides suggest that these interactions are highly specific.

Two of the three trisaccharides (Tri-1 and Tri-3) stimulated proliferation of F32 cells in the presence of acidic FGF (aFGF). However, their potency relative to that of heparin was less than that observed with bFGF (Fig. 1 inset). These data demonstrate that the structure-function relation between heparin/HS and aFGF is similar to that between heparin/HS and bFGF and suggests that recognition of the structural features of heparin/HS is a conserved property of FGFs and is not specific to a single ligand.

FGFs have a high affinity for heparin (binding affinity $K_d = 10^{-9}$ M) (11). We assayed the ability of the synthetic oligosaccharides to compete with the binding of 125 I-labeled heparin to FGF (12). Oligosaccharides Di-3, Di-4, Tri-1, and Tri-3, and the related molecule, SOS, all bound aFGF (9) and bFGF (Fig. 2A and Table 2) (9). Heparin, Tri-1, and Tri-3 bound FGF with an affinity higher than that of SOS. Di-3, Di-4, and SOS bound FGF with similar affinity, whereas Di-2, Tri-2, and Tetra-1 bound bFGF with an affinity less than that of SOS. The number of hydrogen bonds in

Table 1. Heparin/HS oligosaccharides. Abbreviations of structure names are as follows: IdoA, iduronic acid; GlcA, glucuronic acid; GlcN, glucosamine; Gal, galactose; aManOH, 2,5-anhydro-D-mannitol; Ac, acetate; and Me, methyl.

Name	M_r	Structure
Di-1	433.3	α -L-IdoA-(1→4)- α -D-GlcNAc-1→OMe
Di-2	493.2	α -L-IdoA-(1→4)- α -D-GlcNSO ₃ -1→OMe
Di-3	433.3	β -D-GlcA-(1→4)- α -D-GlcNAc-1→OMe
Di-4	493.2	β -D-GlcA-(1→4)- α -D-GlcNSO ₃ -1→OMe
Di-5	433.3	α -D-GlcNAc-(1→4)- β -D-GlcA-1→OMe
Tri-1	631.4	β -D-GlcA-(1→4)- α -D-GlcNAc-(1→4)- β -D-GlcA-1→OMe
Tri-2	691.2	α -L-IdoA-(1→4)- α -D-GlcNSO ₃ -(1→4)- β -D-GlcA-1→OMe
Tri-3	631.4	α -L-IdoA-(1→4)- α -D-GlcNAc-(1→4)- β -D-GlcA-1→OMe
Tetra-1	793.6	α -L-IdoA-(1→4)- α -D-GlcNAc-(1→4)- β -D-GlcA-1-(1→3)- β -D-Gal-1→OMe
Tetra-4*	865.6	α -L-IdoA-(1→4)-6-SO ₃ - α -D-GlcNAc-(1→4)- β -D-GlcA-(1→4)- α -D-aManOH
Tetra-5*	865.6	β -D-GlcA-(1→4)-6-SO ₃ - α -D-GlcNAc-(1→4)- β -D-GlcA-(1→4)- α -D-aManOH

D. M. Ornitz, Department of Molecular Biology and Pharmacology, Washington University Medical School, St. Louis, MO 63110, USA.

A. B. Herr and G. Waksman, Department of Biochemistry and Molecular Biophysics, Washington University Medical School, St. Louis, MO 63110, USA.

M. Nilsson, J. Westman, C.-M. Svahn, Department of Organic Chemistry, Pharmacia AB, S-112 87 Stockholm, Sweden.

*To whom correspondence should be addressed.

*Purified to isomeric homogeneity from nitrous acid-depolymerized heparin (39).

the crystal structures of Di-3 and Tri-3 complexed with FGF (see below) correlate well with these data. The relative binding affinities also correlate well with the mitogenic

activity of these molecules. However, on the basis of the relative affinities for bFGF (Table 2), Di-2, Tri-1, and Tri-3 show higher than expected mitogenic activity. Thus,

factors other than direct binding to bFGF may contribute to the biological activity of these molecules.

Binding of bFGF to a soluble FGFR-alkaline phosphatase fusion protein (FRAP) or to a cell-surface FGFR is enhanced by heparin/HS or by heparin-derived oligosaccharides (8 to 12 sugar residues) (3, 4). We measured the ability of heparin/HS-derived di-, tri-, and tetrasaccharides to enhance FGF-FRAP binding in vitro (3). These studies showed that Di-3, Di-4, and Tri-3 enhanced bFGF-FRAP binding (Fig. 2B). Furthermore, the binding of either aFGF (Fig. 2C) or bFGF (Fig. 2D) to FRAP increased in a dose-dependent manner. At high concentrations of Tri-3, the amount of ¹²⁵I-bFGF bound to FRAP reproducibly exceeded that observed with heparin (Fig. 2D). The observation that small di- and trisaccharides can enhance FGF-FRAP binding suggests that multiple binding sites along a single heparin/HS chain (like beads on a string) are not essential for biological activity, and that the occupancy of a relatively small heparin/HS binding site or sites on FGF may be sufficient to activate FGF. The inability of Tri-1 to enhance FGF-FRAP binding suggests that several mechanisms may mediate FGF receptor activation. Clearly, the substitution of an iduronic acid for a glucuronic acid at the nonreducing end of the saccharide is sufficient to discriminate between different modes of action.

Heparin/HS may stabilize a ternary complex by binding directly to the FGFR (6) in addition to FGF. To investigate this model, we incubated FRAP with ¹²⁵I-heparin (12). No significant binding (more than twofold over background binding) between ¹²⁵I-heparin and FRAP could be detected. However, if bFGF (up to 4 nM) was added to

Fig. 1. Mitogenic activity of synthetic oligosaccharides. Activation of bFGF mitogenic activity as measured by [³H]thymidine incorporation into F32 cells treated with 150 pM bFGF and increasing concentrations of the indicated oligosaccharides. Inset at upper left shows activation of aFGF mitogenic activity determined as above in the presence of 250 pM aFGF. The dashed line at 2 × 10⁴ cpm incorporated was used to calculate the relative mitogenic activity shown in Table 2. These data are representative of at least two independent experiments.

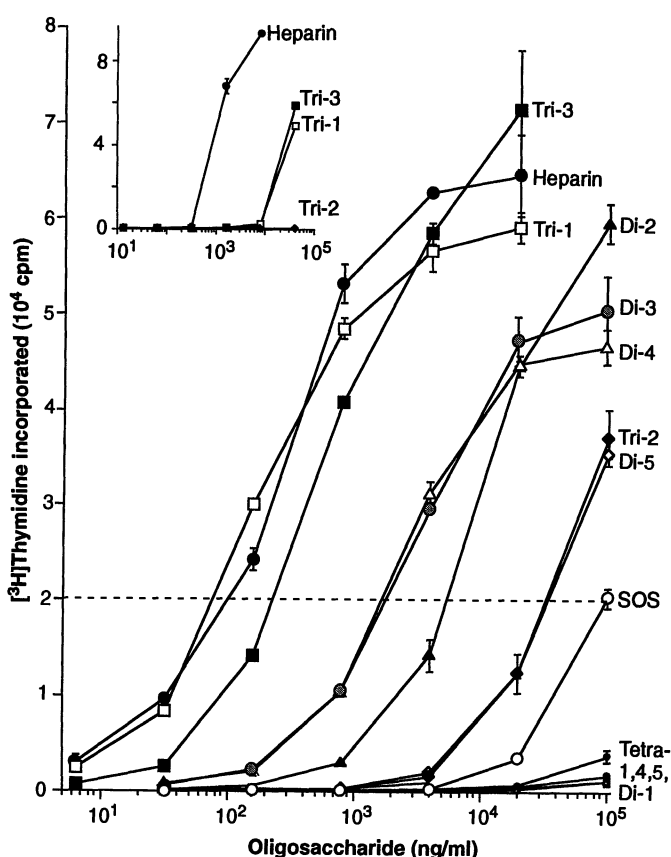


Fig. 2. Biochemical properties of synthetic oligosaccharides. (A) Binding of oligosaccharides to bFGF as determined by competition with ¹²⁵I-heparin is shown (28). The IC₅₀'s (50% competition for ¹²⁵I-heparin binding to bFGF) are: 69 ng/ml for heparin, 11.7 μg/ml for Tri-1, 5.8 μg/ml for Tri-3, and 93 μg/ml for SOS. (B) Binding of ¹²⁵I-bFGF to FRAP in the presence of the indicated oligosaccharide is shown. Dash indicates no heparin added. Heparin was at a concentration of 50 ng/ml; the remaining oligosaccharides were added at a concentration of 2 μg/ml. FGFs were labeled by the Chloramine T method as previously described (37). (C) Acidic and (D) basic FGF binding to FRAP are shown. ¹²⁵I-FGFs were incubated with FRAP in the presence of increasing concentrations of heparin or Tri-3. Binding assays were done as described (3).

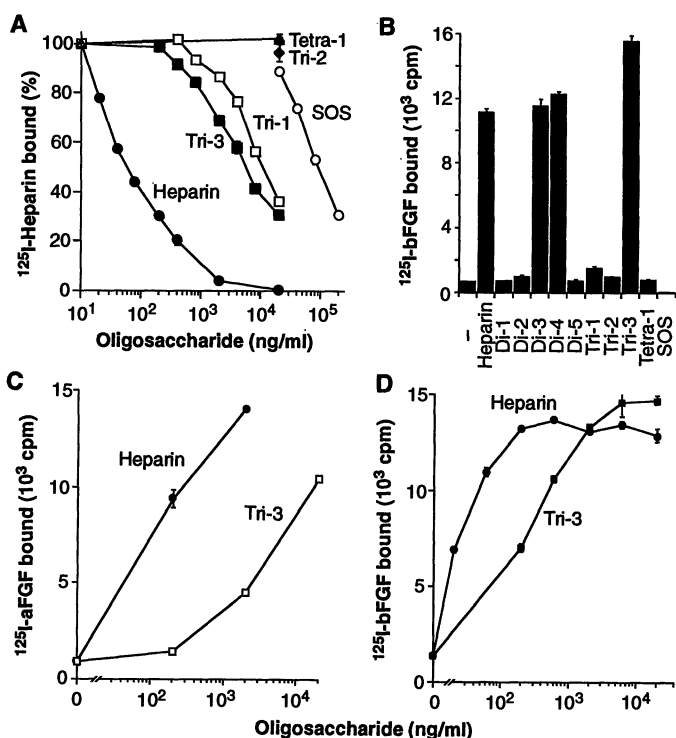


Table 2. Glycosaminoglycan cofactor activity. Mitogenic activity is shown as the relative concentration (w/v) required to incorporate 2 × 10⁴ cpm [³H]thymidine into F32 cell DNA (3), ± SD (see Fig. 1). bFGF binding (see Fig. 2A) is shown as relative affinity [based on IC₅₀ values (w/v)] for heparin binding to bFGF. Calculations based on molecular weights give similar ratios, with the assumption that the average molecular weight for heparin is 16,000 and that there are 15 FGF binding sites per heparin/HS molecule (40).

Name	Mitogenic activity	bFGF binding
Heparin	1.0 ± 0.5	1.0
Di-2	69.5 ± 9.6	>1340.6
Di-3	26.0	1224.5
Di-4	24.7	1224.5
Di-5	463.6	>1340.6
Tri-1	1.2 ± 0.2	169.3
Tri-2	470.6 ± 25.6	>1340.6
Tri-3	3.2	84.1
SOS	1380.8 ± 30.6	1340.6

this binding reaction, ^{125}I -heparin binding was increased up to 25.5-fold over background (13). These data and the observation that molecules as small as disaccharides were biologically active suggest that the mechanism by which heparin/HS activates the FGFR results from a primary interaction between the FGFR and a complex of heparin/HS and FGF.

To further evaluate the mechanism by which heparin/HS activates FGF and to establish a framework for the rational de-

sign of drugs that modulate the activity of FGF, we determined the crystal structure of complexes between bFGF and biologically active di- and trisaccharides (14) (Fig. 3A). A view of a molecule of bFGF with bound Di-3 reveals four binding sites (Fig. 3B). Similar observations were made with the Tri-3-bFGF complex (Fig. 3, C and D). Bound and apo-FGF structures superimpose with a root-mean-square deviation in $\text{C}\alpha$ positions of 0.26 Å. It is therefore unlikely that a conformational change in FGF is

involved in its mechanism of activation by heparin.

Two ligand molecules were observed in the crystal structure. Each ligand contacted two symmetry-related FGF molecules, thus defining two pairs of binding sites: 1 and 1' and 2 and 2' (Fig. 3B). Site 1 is similar to that observed for SOS bound to aFGF (15) and is also the site where sulfate ions are located in the bFGF apo-structure (16–18). Twelve hydrogen bonds, as defined in (19), formed between FGF and Tri-3 at site 1. In

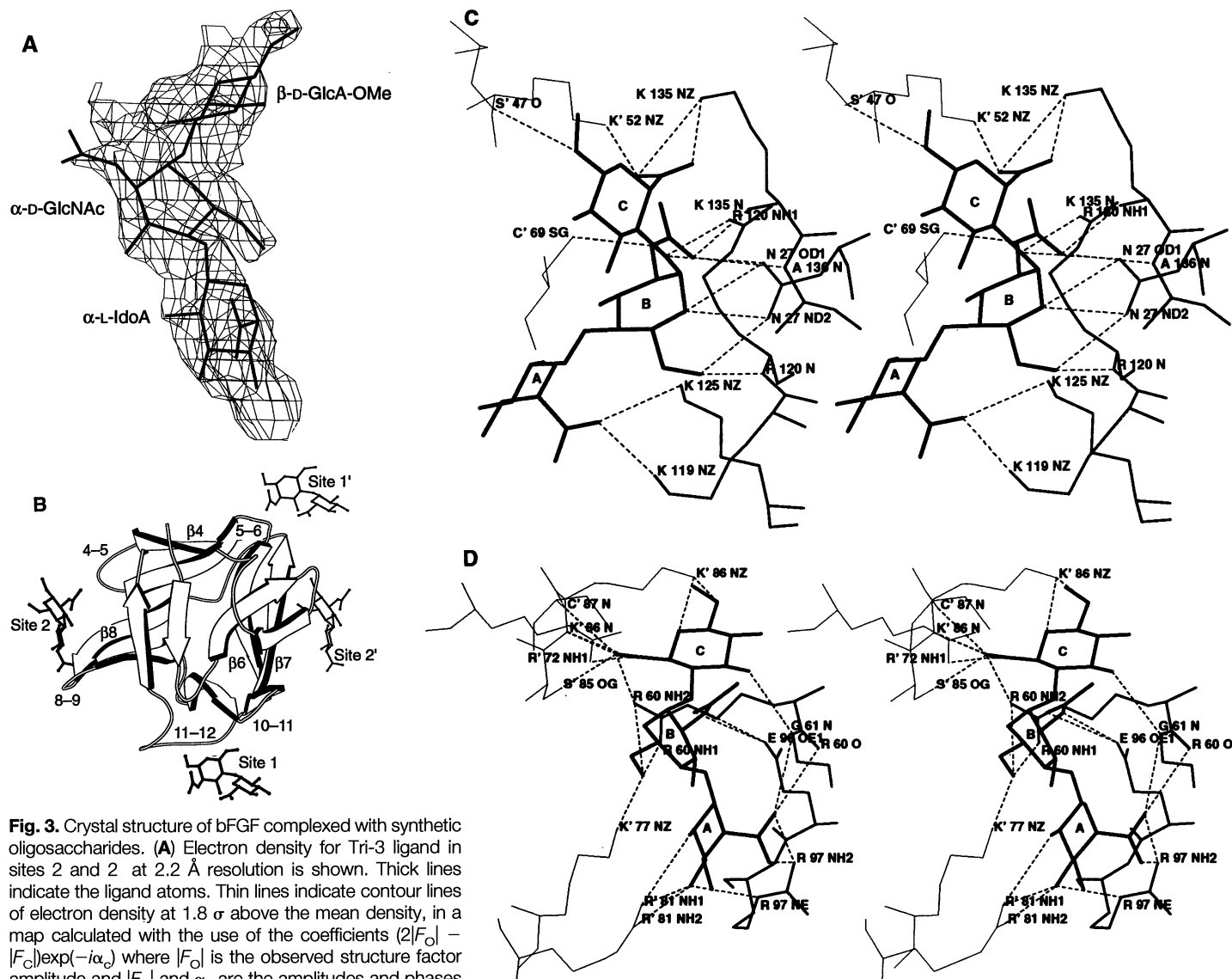


Fig. 3. Crystal structure of bFGF complexed with synthetic oligosaccharides. **(A)** Electron density for Tri-3 ligand in sites 2 and 2' at 2.2 Å resolution is shown. Thick lines indicate the ligand atoms. Thin lines indicate contour lines of electron density at 1.8σ above the mean density, in a map calculated with the use of the coefficients $(2|F_{\text{O}}| - |F_{\text{C}}|)\exp(-i\alpha_{\text{C}})$ where $|F_{\text{O}}|$ is the observed structure factor amplitude and $|F_{\text{C}}|$ and α_{C} are the amplitudes and phases calculated from the model and adjusted by addition of the structure factor of the solvent (14). Sugar residues are abbreviated as shown in Table 1. **(B)** Ribbon diagram (38) of bFGF bound to Di-3 molecules, shown with solid black bonds and labeled according to the sites to which they bind. The prime mark refers to symmetry-related molecules. The β strands are shown as arrows. The notation used is according to (17), with strands labeled from $\beta 1$ to $\beta 12$ and loops labeled with the numbers of the secondary structures they join. Only secondary structures participating in the Di-3-bFGF interaction are indicated. However, the location and features of the Tri-3 binding sites are essentially the same. **(C)** Stereodiagram of sites 1 and 1' with the Tri-3 ligand at a dimer interface. Tri-3 is shown with thick, solid black bonds. Sugar rings are labeled A, B, and C, with A indicating iduronic acid, B indicating *N*-acetylglucosamine, and C indicating

O-methylglucuronic acid. Medium-thick and thin lines indicate amino acid atoms involved in sites 1 and 1', respectively. Dotted lines indicate hydrogen bonds. Atoms and amino acids involved in hydrogen bonds are indicated by a prime mark when the bond involves atoms of site 1'. The oligosaccharide in site 1 is within a pocket of high positive electric potential that includes primarily amino acids of the 10–11 and 11–12 loops [see (B) for notation]. Site 1' makes contacts with regions of the structure that include the 5–6 loop and the $\beta 4$ strand. **(D)** Stereodiagram of sites 2 and 2' with the Tri-3 ligand at a dimer interface. Notation is as in (C). Site 2 consists of regions of the structure that include the $\beta 8$ strand and the 4–5 loop. Site 2' consists of a largely hydrophobic platform (strands $\beta 6$ and $\beta 7$) flanked by positively charged residues Arg⁷² and Lys⁸⁶ on one side and residues Arg⁸¹ and Lys⁷⁷ on the other side.

comparison, only three hydrogen bonds formed at site 1' (Fig. 3C). These data suggest that sites 1 and 1' are not equivalent in terms of binding affinity and therefore are unlikely to be involved in FGF oligomerization. Site 1' most likely results from crystal packing forces.

Sites 2 and 2' (Fig. 3, B and D) have not been observed previously. This pair of sites is symmetry-related and consequently located very close to a crystal packing interface. In contrast to sites 1 and 1', both symmetry-related FGF molecules made extensive contact with Tri-3 at sites 2 (11 hydrogen bonds) and 2' (11 hydrogen bonds). Therefore, each of these sites is likely to bind ligand with high affinity, and each can be considered an independent binding site. However, the average hydrogen bond length between Tri-3 and site 2' was 0.35 Å shorter than that between Tri-3 and site 2. In addition, if a more stringent definition of the hydrogen bond was used (20), eight hydrogen bonds were observed between Tri-3 and site 2' as compared with only four between Tri-3 and site 2. This indicates that site 2' may have greater affinity for Tri-3 than does site 2. In the crystal structure, site 2 of one FGF molecule and site 2' of a symmetry-related FGF molecule are brought together by a single oligosaccharide molecule. Such contacts may be responsible for the oligomerization of FGF (see crosslinking experiments below).

Several other putative heparin/HS binding sites on bFGF have been suggested (21, 22); however, no density was observed at these sites for either Di-3 or Tri-3. In contrast to SOS, which has minimal biological activity and occupies a single site on the aFGF molecule, multiple binding sites for

Di-3 and Tri-3 were observed. The capability of di- and trisaccharides to bind several sites on FGF may be a requirement for activity. Additionally, these sites may represent a path followed by heparin/HS polysaccharides between two FGF molecules complexed in a functional dimer. Although the biological relevance of the potential dimer interface at site 2-2' remains to be proven, cross-linking studies demonstrate that both di- and trisaccharides can induce FGF oligomerization.

Di-3 and Tri-3, like the highly sulfated heparin hexadecasaccharide (HS-16), can induce FGF dimers as well as higher order oligomers (Fig. 4) (3). However, there are notable differences between the synthetic oligosaccharides and HS-16. The optimal concentration for dimerization activity induced by Tri-3 (35 µg/ml) is approximately 10 times greater than that of HS-16 (3.9 µg/ml). At concentrations 10 to 20 times greater than these, the amount of dimerization seen with the hexadecasaccharide approaches basal levels. However, the amount of dimerization seen with the di- (13) or trisaccharide (Fig. 4) remains elevated. High ratios of HS-16 to FGF may favor a stoichiometry of several heparin oligosaccharides per FGF. Under these conditions, FGF dimerization may be inhibited sterically by the relatively large heparin molecule (HS-16). High ratios of di- or trisaccharide to FGF would not be expected to sterically inhibit FGF dimerization.

The data presented here demonstrate that both nonsulfated di- and trisaccharides are biologically active in several FGF-dependent assays and suggest that FGF can specifically recognize structural features of the nonsulfated carbohydrate backbone of heparin/HS, independent of ionic interactions with highly charged sulfate groups. However, because heparin is more active than low-sulfated heparin (4), it is likely that ionic interactions could further stabilize this interaction. The lack of activity of Tri-2, a compound that only differs from Tri-3 (our most active compound) in having a *N*-sulfate group on the glucosamine residue, suggests that *N*-sulfated regions of heparin/HS may not be involved in FGFR activation. Substitution of an *N*-sulfate in the Tri-3-bFGF crystal structure demonstrates repulsive interactions between the sulfate group and glutamic acid 96 in site 2. Several studies demonstrate that 2-O-linked sulfate groups on the hexuronic acid residues of heparin/HS may be important for optimal activity (23–26). Sulfation of our synthetic oligosaccharides at the 2-O position may further increase their affinity for bFGF and their biological activity.

The small size of the synthetic heparin/HS molecules suggests that linkage of multiple FGFs by heparin/HS in a "beads on a

string" model is not an essential component of the mechanism of FGFR activation. We suggest a mechanism in which heparin/HS induces FGF dimers, which in turn form stable complexes with FGF receptor molecules facilitating receptor dimerization. Recent binding studies, with the use of distinct members of the FGF family, suggest that an FGFR may contain multiple, partially overlapping binding sites that involve both immunoglobulin-like domains II and III (27). These data are consistent with FGFR molecules interacting with homo- or heterodimers of FGF.

REFERENCES AND NOTES

1. C. Basilico and D. Moscatelli, *Adv. Cancer Res.* **59**, 115 (1992).
2. M. Klagsbrun and A. Baird, *Cell* **67**, 229 (1991).
3. D. M. Ornitz *et al.*, *Mol. Cell. Biol.* **12**, 240 (1992).
4. A. Yayon *et al.*, *Cell* **64**, 841 (1991).
5. A. C. Rapraeger, A. Krufka, B. B. Olwin, *Science* **252**, 1705 (1991).
6. M. Kan *et al.*, *ibid.* **259**, 1918 (1993).
7. M. Ishihara *et al.*, *J. Biol. Chem.* **268**, 4675 (1993).
8. B. Casu, in *Heparin and Related Polysaccharides: Structure and Activities*, F. A. Ofofo, I. Danishefsky, J. Hirsh, Eds. (New York Academy of Sciences, New York, 1989), vol. 556, pp. 1–17.
9. J. Westman, M. Nilsson, D. M. Ornitz, C.-M. Svahn, *J. Carbohydr. Chem.* **14**, 95 (1995).
10. J. Folkman *et al.*, *Ann. Surg.* **214**, 414 (1991).
11. D. Moscatelli, *J. Cell. Phys.* **131**, 123 (1987).
12. Heparin iodination was as in (28). Heparin binding to FGF was determined by incubation of 4 nM FGF with ¹²⁵I-heparin and competitor polysaccharide. Complexes were immunoprecipitated with 1:250 dilutions of monoclonal antibody DG2 (for bFGF) or a polyclonal antibody (for aFGF) and protein A-Sepharose (Sigma). Washing and quantitation were as previously described for soluble receptor binding assays (3).
13. D. M. Ornitz, unpublished data.
14. Small crystals of complexes of bFGF (25 mg/ml) and Di-3 or Tri-3 (1 to 1.3 ratios) were obtained at 20°C (29) in 15 or 17.5% (w/v), respectively, polyethylene glycol (average $M_n = 3350$) and 0.1 M HEPES (pH 6.8) and subsequently macroseeded repeatedly in fresh drops of the same solution. Both complexes formed triclinic crystals with one molecule in the asymmetric unit ($a = 30.9$, $b = 33.3$, $c = 34.7$, $\alpha = 87.6$, $\beta = 85.4$, $\gamma = 76.4$). Structure determination was carried out as in (30, 31) with the model generated by (18). The oriented model was then refined by simulated annealing and least-squares optimization, as in (32). Data from 40 to 2.2 Å were used. Examination of a map generated with the use of the coefficients $(|F_o| - |F_c|)\exp(-\alpha_c)$ showed density that could accommodate saccharide molecules in both sites 1 and 2. Subsequent incorporation of the structure factor of the solvent resulted in improved density. Model-building and correction was carried out with the programs O (33, 34) and TURBO (35). Least-squares refinement of the saccharide-FGF structure was carried out with X-PLOR (36), with stereochemical parameters for Di-3 and Tri-3 taken from the topology and parameter files provided for pyranoside sugars by the X-PLOR package (36). The final *R* factor was 22.0 and 22.8% for the Tri-3-bFGF and Di-3-bFGF structures, respectively, with good stereochemistry. Analysis of the temperature factors indicated that the occupancy of the saccharides was likely to be partial. Occupancy of the di- and trisaccharide was set to 0.5, which resulted in temperature factors that were comparable to those for side chains observed to coordinate the ligands.
15. X. Zhu, B. T. Hsu, D. C. Rees, *Structure* **1**, 27 (1993).
16. J. Zhang, L. S. Cousins, P. J. Barr, S. R. Sprang, *Proc. Natl. Acad. Sci. U.S.A.* **88**, 3446 (1991).
17. X. Zhu *et al.*, *Science* **251**, 90 (1991).
18. A. E. Eriksson, L. S. Cousins, L. H. Weaver, B. W.

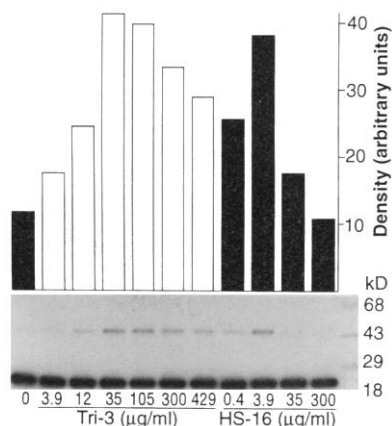


Fig. 4. Dimerization of bFGF in the presence of heparin or synthetic oligosaccharides. 670 nM bFGF and 3×10^5 cpm of ¹²⁵I-bFGF were incubated with the indicated concentrations of heparin oligosaccharide. Cross-linking and electrophoresis were done as described (3). Dimer (45 kD) band intensities were quantified by scanning densitometry and are plotted above each lane.

- Matthews, *Proc. Natl. Acad. Sci. U.S.A.* **88**, 3441 (1991).
19. I. K. McDonald and J. M. Thornton, *J. Mol. Biol.* **238**, 777 (1994).
 20. E. N. Baker and R. E. Hubbard, *Prog. Biophys. Mol. Biol.* **44**, 97 (1984).
 21. A. Baird, D. Schubert, N. Ling, R. Guillemin, *Proc. Natl. Acad. Sci. U.S.A.* **85**, 2324 (1988).
 22. W. F. Heath, A. S. Cantrell, N. G. Mayne, S. R. Jaskunas, *Biochemistry* **30**, 5608 (1991).
 23. S. Guimond, M. Maccarana, B. B. Olwin, U. Lindahl, A. C. Rapraeger, *J. Biol. Chem.* **268**, 23906 (1993).
 24. M. Maccarana, B. Casu, U. Lindahl, *ibid.*, p. 23898.
 25. H. Habuchi *et al.*, *Biochem. J.* **285**, 805 (1992).
 26. D. Aviezer *et al.*, *J. Biol. Chem.* **269**, 114 (1994).
 27. A. T. Chellaiah, D. G. McEwen, S. Werner, J. Xu, D. M. Ornitz, *ibid.*, p. 11620.
 28. C. G. Glabe, P. K. Harty, S. D. Rosen, *Anal. Biochem.* **130**, 287 (1983).
 29. A. McPherson, *Eur. J. Biochem.* **189**, 1 (1990).
 30. M. G. Rossmann, in *International Scientific Review Series* (Gordon and Breach, New York, 1972), vol. 13.
 31. A. T. Brünger, *Acta Crystallogr.* **46**, 46 (1990).
 32. W. I. Weiss, A. T. Brünger, J. J. Skehel, D. C. Wiley, *J. Mol. Biol.* **212**, 737 (1990).
 33. T. A. Jones and S. Thirup, *EMBO J.* **5**, 819 (1986).
 34. T. A. Jones, J. Y. Zou, S. W. Cowan, M. Kjeldgaard, *Acta Crystallogr.* **47**, 110 (1991).
 35. A. Roussel and C. Cambillau, TURBO-FRODO, in *Silicon Graphics Geometry Partners Directory* (Silicon Graphics, Summit, NJ, 1991), p. 86.
 36. A. T. Brünger, *X-PLOR Manual, Version 3.1* (Yale University, New Haven, CT, 1992).
 37. L. W. Burrus and B. B. Olwin, *J. Biol. Chem.* **264**, 18647 (1989).
 38. P. J. Kraulis, *J. Appl. Crystallogr.* **24**, 946 (1991).
 39. C. Svahn, A. Ansari, T. Wehler, unpublished data.
 40. H. Mach *et al.*, *Biochemistry* **32**, 5480 (1993).
 41. We thank D. McEwen and S. Matthews for discussion and A. Chellaiah, T. Opera, J. Xu, and M. Weurffel for help. The bFGF and antibody DG2 were gifts from J. Abraham (Scios Nova) and W. Herblin (DuPont-Merck), respectively. The aFGF and the aFGF antiserum were a gift from K. Thomas (Merck). Fluoresceinated heparin was a gift from C. Parish (Australian National University, Canberra, Australia). SOS was from Bukh Meditec. Heparin was from Hepar Inc. Supported in part by grants from NIH (CA60673), Monsanto-Searle, the Beckman Young Investigators Program (D.M.D.), and Washington University Medical School.

4 October 1994; accepted 5 January 1995

Measurement of Interhelical Electrostatic Interactions in the GCN4 Leucine Zipper

Kevin J. Lumb and Peter S. Kim*

The dimerization specificity of the bZIP transcription factors resides in the leucine zipper region. It is commonly assumed that electrostatic interactions between oppositely charged amino acid residues on different helices of the leucine zipper contribute favorably to dimerization specificity. Crystal structures of the GCN4 leucine zipper contain interhelical salt bridges between Glu²⁰ and Lys^{15'} and between Glu²² and Lys^{27'}. ¹³C-nuclear magnetic resonance measurements of the glutamic acid pK_a values at physiological ionic strength indicate that the salt bridge involving Glu²² does not contribute to stability and that the salt bridge involving Glu²⁰ is unfavorable, relative to the corresponding situation with a neutral (protonated) Glu residue. Moreover, the substitution of Glu²⁰ by glutamine is stabilizing. Thus, salt bridges will not necessarily contribute favorably to bZIP dimerization specificity and may indeed be unfavorable, relative to alternative neutral-charge interactions.

Transcription factors of the basic-region leucine zipper (bZIP) family bind to DNA as homo- or heterodimers (1). Dimerization of these proteins is controlled by the leucine zipper (Fig. 1A), a parallel, two-stranded coiled coil (2-4). The leucine zipper thus mediates the DNA-binding specificity of the bZIP transcription factors by determining which bZIP proteins form stable dimers. Accurate prediction of bZIP dimerization specificity will require an understanding of the principles governing leucine zipper dimerization.

The formation of favorable hydrophobic packing interactions involving residues at positions a and d of the coiled-coil heptad repeat, and including the side chains of res-

idues at positions e and g (Fig. 1B), can contribute to dimerization specificity. Residues at the e and g positions also can contribute substantially to the specificity of leucine zipper dimerization through interhelical electrostatic interactions (Fig. 1A). Previous studies have demonstrated that the dimerization specificity of both the Fos-Jun oncoprotein (5) and a de novo designed heterodimeric coiled coil (6) results largely from the relief of unfavorable interhelical electrostatic interactions between residues of like charge in the homodimers. Thus, avoidance of electrostatic repulsion is an important determinant of dimerization specificity (5, 6).

Conversely, it is often assumed that formation of favorable electrostatic interactions between the helices contributes to the global stability and dimerization specificity of two-stranded coiled coils (4, 7-12). Indeed, crystal structures of leucine zippers (4,

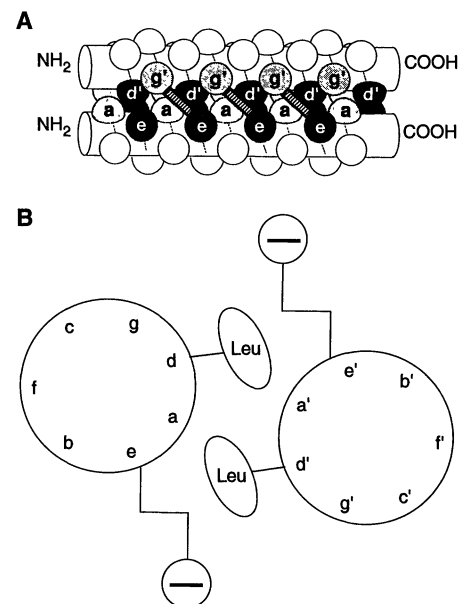


Fig. 1. (A) Schematic representation of the leucine zipper, a parallel, two-stranded coiled coil (4). A side view is shown. For simplicity, the supercoiling of the helices is not depicted. The sequences of coiled coils are characterized by a heptad repeat of seven amino acid residues, denoted a to g (7). Prime (') refers to positions from the other helix. Most of the residues at positions a and d are hydrophobic, forming the characteristic 4-3 repeat of coiled coils, whereas residues at positions e and g are often charged (7, 26). The hydrophobic interface between the two α helices is formed by residues at positions a, d, e, and g (4). One set of packing interactions consists of side chains from positions a, a', g and g' (light shading), whereas the second set consists of side chains from positions d, d', e, and e' (dark shading). Residues at positions g' and e pack against positions a and d', respectively, and can participate in interhelical electrostatic interactions with position e to g' of the preceding heptad (indicated with ladders). (B) Schematic cross section through the dimer, depicting packing interactions between the residues at positions d and e (4). As an example, leucine at position d and glutamic acid at position e is shown. The large circles represent the helical backbone and the line segments represent bonds between carbon atoms. Residues at d and d' make side-to-side interactions. Additionally, methylene groups from residues at positions e and e' make contacts with the hydrophobic residues at positions d and d'. These types of interactions are also present in the a layer, in which residues from positions g and g' make contacts with residues at positions a and a'.

10, 11) show interhelical salt bridges between charged residues at g' positions to residues of opposite charge, on the other helix, at e positions of the following heptad (Fig. 1A).

GCN4-p1 is a synthetic peptide corresponding to the leucine zipper of the yeast transcriptional activator GCN4 (Fig. 2A). Interhelical salt bridges are observed in the crystal structure of GCN4-p1 (13) between

Howard Hughes Medical Institute, Whitehead Institute for Biomedical Research, Department of Biology, Massachusetts Institute of Technology, Nine Cambridge Center, Cambridge, MA 02142, USA.

*To whom correspondence should be addressed.